MRS Advances © 2020 Materials Research Society
DOI: 10.1557/adv.2020.295

Oxides and the high entropy regime: A new mix for engineering physical properties

P. B. Meisenheimer[1] and J. T. Heron[1]

[1] *University of Michigan, Department of Materials Science and Engineering, 2300 Hayward St, Ann Arbor, MI, USA, 48109*

ABSTRACT

Historically, the enthalpy is the criterion for oxide materials discovery and design. In this regime, highly controlled thin film epitaxy can be leveraged to manifest bulk and interfacial phases that are non-existent in bulk equilibrium phase diagrams. With the recent discovery of entropy-stabilized oxides, entropy and disorder engineering has been realized as an orthogonal approach. This has led to the nucleation and rapid growth of research on high-entropy oxides – multicomponent oxides where the configurational entropy is large but its contribution to its stabilization need not be significant or is currently unknown. From current research, it is clear that entropy enhances the chemical solubility of species and can realize new stereochemical configurations which has led to the rapid discovery of new phases and compositions. The research has expanded beyond studies to understand the role of entropy in stabilization and realization of new crystal structures to now include physical properties and the roles of local and global disorder. Here, key observations made regarding the dielectric and magnetic properties are reviewed. These materials have recently been observed to display concerted symmetry breaking, metal-insulator transitions, and magnetism, paving the way for engineering of these and potentially other functional phenomena. Excitingly, the disorder in these oxides allows for new interplay between spin, orbital, charge, and lattice degrees of freedom to design the physical behavior. We also provide a perspective on the state of the field and prospects for entropic oxide materials in applications considering their unique characteristics.

INTRODUCTION

High-entropy materials, popularized by the discovery of high-entropy metal alloys ~20 years ago[1–4], typically include 5 or more atomic species and are kinetically frozen into a metastable solid solution phase that is stable at high temperature[5,6]. These materials are characterized by both rule-of-mixtures and cocktail effect behavior and are nominally disperse on an atomic scale[1,7,8]. In an entropy-stabilized material, the configurational entropy contribution to the Gibbs' free energy drives the formation of a single phase solid solution[2,9], potentially even in excess of a positive enthalpy of formation[9]. High-entropy and entropy-stabilized oxides (HEOs and ESOs) have attracted significant interest due to the apparent deviations from Gibbs' phase rule and the prospect for increased hardness, toughness, corrosion resistance, and thermal resistance[6,10]. Prior to the seminal work in 2015 that nucleated the HEO field[9], there were only a few reports exploring high-entropy transition metal nitrides as an extension of the HEA community[11–13], however investigations outside of transition metal alloys have recently begun to explode. **Figure 1a** plots the number of publications on the topic which were found using title keywords "high-entropy" or "entropy-stabilized" and "oxides" or "ceramics" in *Web of Science*. The number of publications has increased exponentially since the field's inception and is a clear indicator of the excitement for and potential impact of entropic materials. In this review, we highlight some of the reasons for this excitement using published findings, opens questions, and a perspective of the future field.

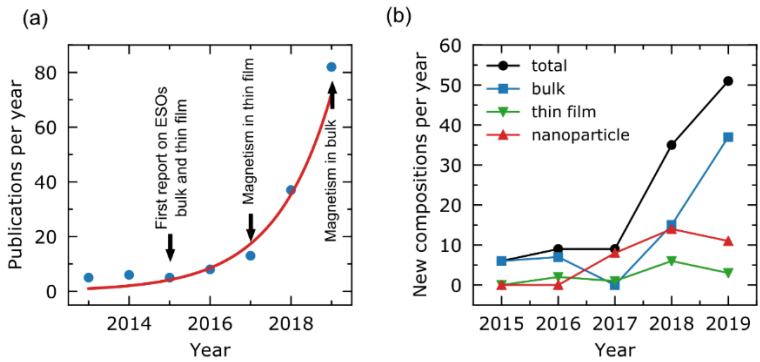

Figure 1: (a) Publications per year using title keywords "high-entropy" or "entropy-stabilized" and "ceramics" or "oxides" retrieved from *Web of Science*. The red line is a fit of the data to an exponential function. **(b)** Number of new high entropy oxide compositions over time and broken down by synthesis method. Data for part **(b)** is from ref [14], compositions with 3 components or less are not counted.

In high-entropy materials, the stability may be influenced by the entropy of mixing (ΔS in $\Delta G = \Delta H - T\Delta S$), potentially even overriding a positive enthalpy of mixing in entropy-stabilized materials. Pioneering work by Rost et al.[9] showed that the multicomponent entropy-stabilized rocksalt oxide (MgCoNiCuZn)O emerges as a solid solution from a phase separated rocksalt-spinel mixture at high temperatures. The evidence for entropic stabilization comes from 3 main observations. 1. The experimental transition temperature of this phase change follows the resulting change in entropy as the relative compositions of the constituent elements are varied. 2. The phase change is reversible and endothermic. 3. The entropy-stabilized phase is chemically homogeneous. In the same study, it has been observed that typically immiscible concentrations of cationic species can be dissolved into the crystal, relative to the binary parent compounds, and place cationic species into atypical coordination. **Figure 2a** illustrates this observation for the case of (MgCoNiCuZn)O, where the solubility of Cu^{2+} and Zn^{2+} is enhanced in the ESO rocksalt crystal where they are octahedrally coordinated in contrast to the tetrahedral coordination of their equilibrium binary phases. The ability to realize new phases and stereochemistry, along with disorder, has opened new space for the synthesis and design of oxide materials.

UNIQUE FEATURES AND PROSPECTS FOR HIGH-ENTROPY OXIDES

Initial (MgCoNiCuZn)O entropy-stabilized oxides studied by Rost et. al., were synthesized by traditional solid-state methods (mill, press, sinter), with thermodynamic stabilization of the equimolar phase occurring at approximately 900 °C and air quenching back to room temperature to preserve the high temperature phase[9]. Bulk synthesis has since been extended to a number of compositions and remains the most pervasive synthesis method of HEOs at this time (**Figure 1b**). Since the entropic contribution to the free energy is temperature dependent, it follows that the higher the temperature at which the crystal is sintered, the larger the driving force for stabilization. Further, these materials must be rapidly quenched from high temperature to maintain the phase at room temperature. For this reason, nanoparticle formation and thin films synthesized by plasma based physical vapor deposition (PVD) have yielded compositions not achievable in bulk, due to increased effective temperatures and quench rates from size effects and plasma condensation respectively[15–18].

As the number of new material compositions has increased dramatically, the number of thin film reports have grown at a much slower rate (**Figure 1b**). While films are the least represented in the literature currently, we do not see this as the case moving forward. In the same initial work by Rost et al., it was demonstrated that single crystal thin films of (MgCoNiCuZn)O could be deposited on (001)-oriented MgO substrates by pulsed laser deposition (PLD)[9], which was later further corroborated by other groups[19,20]. Despite the large estimated strains (up to ~4.5% in some cases[19]) and anticipated lattice disorder, (MgCoNiCuZn)O and compositional variant films on MgO substrates are incredibly high quality. The films show robust Kessig fringes[18,19,21], commensurate epitaxy to the substrate[19,21], chemical homogeneity down to resolution by STEM EDS[9], and rocking curves as narrow as that of the underlying substrate[9,19]. In this vein, a significant advantage of HEOs remains their structural tunability[19,22–24] and, at least for ESOs, the ability to be grown on a variety of substrates[15,25], including amorphous materials, resulting in substrate versatility for potential applications. A laser ablation

deposition study by Kotsonis and colleagues observed that the kinetic energy of species (1s-10s of eV, T_{eff} ~10^4-10^5 K) dictated whether the film was in the ESO phase or the phase separated rocksalt-spinel mixture[15]. The metastable ESO rocksalt phase was found to favor the deposition conditions associated with large kinetic energies. Their findings suggest that the extreme kinetic energy and quenching associated with PVD deposition will further open the composition space for ESOs relative to near-equilibrium bulk techniques. Indeed, it has been experimentally observed that some compositions are able to be stabilized as thin films, but not as bulk material[15,18]. Thus, thin films broaden the stabilization space, can be deposited on a wide variety of substrates, and the need for a large effective quench favors the low temperature deposition for BEOL (back-end of line) compatibility.

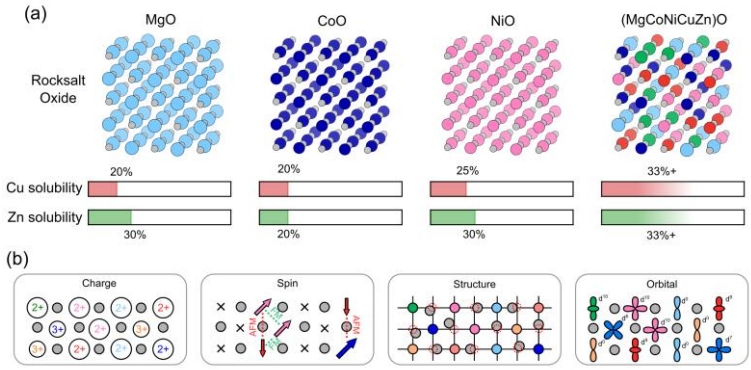

Figure 2: (a) Illustration of the enhanced solubility of cations into ESOs. The solubility of Cu and Zn, both cations with different preferred coordination (tetrahedral) and crystal structure (tenorite and wurtzite, respectively), are shown by the solubility bars for the binary rocksalt and ESO solvent systems. The solubility is significantly enhanced in the ESO. Even more so, the phase diagram of (MgCoNiCuZn)O has not been investigated, so the solubility limit may be even higher than yet reported[9]. The solubilities given are taken from bulk phase diagrams[26–30] at 1000 °C, the approximate stabilization temperature of (MgCoNiCuZn)O with ~33% Cu or Zn. **(b)** Illustration of the disorder in HEOs, where new properties can be engineered and tuned using the interplay between local charge, spin, structural, and orbital degrees of freedom.

As a result of the enhanced solubility of ESOs, the crystal can be stabilized with competing internal charge, spin, structure, and orbital order/disorder that develop physical or functional frustrations (**Figure 2b**), e.g. the structural distortion caused by Jahn-Teller active Cu^{2+} in rock-salt (MgCoNiCuZn)O[21,31,32]. By understanding and controlling the enhanced solubility of these materials, charge, spin, lattice, and orbital degrees of freedom new properties are envisioned. For instance, the structural distortions caused by Jahn-Teller active Cu^{2+} can drive oxidation state changes in other cations, which in turn effects the spin-dependent properties[31]. Existing techniques for the study and synthesis of thin-film correlated oxides such as multiferroics[33,34], spin ices and liquids[35–38], and superconductors[39–41] take advantage of a number of thin film paradigms such as layer-by-layer growth[42] and interfacial control[43–46] making tunability and precise

control of structure and stereochemistry critically important. Fabrication of these materials is also solubility limited, as the chemical composition can only be engineered within the allowed enthalpies of mixing. This presents an interesting opportunity for the exploration of correlated entropy-stabilized oxides, as not only does the structure appear to be robust and controllable to an unprecedented level, but entropy-stabilization vastly increases the composition space where materials can be discovered. This significant tunability of structure and chemistry coupled with recent observations of functionality in these materials[31,47,48] opens opportunities for studying the interplay between charge, spin, lattice, and orbital degrees of freedom and engineering of physical behavior in highly disordered crystalline materials. For the remainder of this article, we focus on summarizing the research in the field related to these ideas with a primary focus on dielectric and magnetic behavior.

DISORDER DRIVEN PROPERTIES

Dielectricity and charge-lattice coupling

Dielectric and ferroelectric oxides have long been a group of technologically relevant materials that have a unique relationship with chemical disorder. In many cases, it is desirable for these materials to exist in a very precipitous phase space to maximize the ferroelectric and piezoelectric response. This is often done through chemical substitution in lead-based perovskites such as PZT ($Pb(ZrTi)O_3$), PZN ($Pb(ZrNb)O_3$), and PMN-PT ($Pb(MnNb)O_3$-$PbTiO_3$) to promote competition between ferroelectric phases and/or crystalline phases[49–52]. This is desirable because lattice softening at the phase boundary increases the polarizability and charge-lattice coupling of the crystal, and local chemistry can modify the phase stability of the oxide[53,54]. Recently, modern techniques such as diffuse neutron scattering, a technique able to probe local, inelastic scattering events, has been used to show the even more important role of disorder in relaxor ferroelectrics due to the formation of polar nanoregions (PNR)[55]. PNR form due to frustration from competing ferroelectric orders in the material (**Figure 3**) that significantly increase the piezoelectric response of the crystal due to coupling with lattice phonons[49,56] and polarization of the nearby ferroelectric matrix[57]. These two effects, phase instability and frustrated ferroic orders, are clear possibilities in high entropy oxides where the material can conceivably be made from constituent species with differing preferred crystal structures and ferroic orders, while being coerced into a metastable phase by entropy. Illustrated in **Figure 3(d)**, the inclusion of Jahn-Teller active Cu^{2+} cations works to create local structural distortions because of the frustrated stereochemistry. This results in a crystal that is disordered on an atomic scale, potentially allowing contributions to a dielectric response. This effect has been explored further in regards to the magnetism of the oxides[31], which will be discussed further below.

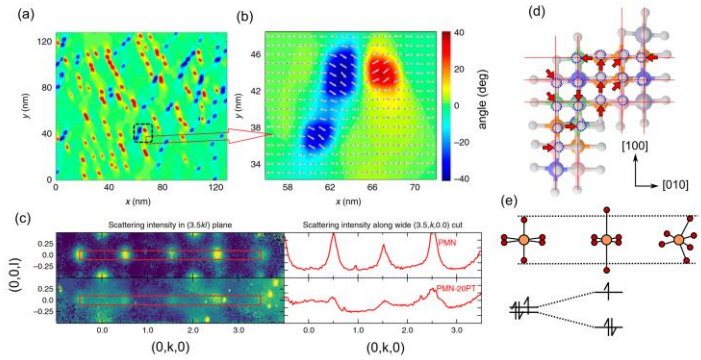

Figure 3: (a) and (b) Phase field simulation of polar nanoregions arising in PMN-PT due to frustration from antiferroelectric and ferroelectric orders. The PNR show up as polar particles that are separate from the ferroelectric matrix, which couple to it to increase local polarizability. **(c)** Diffuse neutron scattering data showing the local antiferroelectric response in PMN-PT, demonstrating experimentally that relaxor behavior is a result of competition between ferroelectric and antiferroelectric orders. **(d)** DFT calculated structure showing the random structural disorder and lattice frustration of (MgCoNiCuZn)O, where the distortions of the oxygen atoms from the ideal planes (red lines) are highlighted by the red arrows. **(e)** Illustration showing an intuitive guide to how the Jahn-Teller distortion of Cu^{2+} creates structural defects in the crystal. Parts **(a,b)** from ref [57]. Part **(c)** from ref [49]. Part **(d)** from ref [31].

The extreme tunability of the structural lattice in rocksalt ESOs has been demonstrated[31,32,58] with the systematic inclusion of Jahn-Teller active species into rocksalt (MgCoNiCuZn)O, where the inclusion of Cu^{2+} cations works to frustrate the stereochemistry. This effect generates disorder on local and global scales, observable through density functional theory simulations[31,32] (**Figure 4(a,b)**), analysis of bulk diffraction intensities[58] (**Figure 4(c)**), and local scattering effects[31]. Particularly in bulk ceramics, the Jahn-Teller effect imparts a rhombohedral or tetragonal distortion to the lattice, which is seen as a decrease in intensity of the highest symmetry ({200} planes) diffraction peaks, which will be most strongly affected as local symmetry is lowered. Beyond investigations of the parent rocksalt, structural tunability has also been observed in perovskite HEO Ba(ZrSnTiHfNb)O_3, which is subject to random structural distortions due to competing cation sizes[24] and possible preferred local coordinations. The component phases are a selection of competing displacive ferroelectric ($BaTiO_3$) and well known paraelectric ($BaZrO_3$, $BaHfO_3$) oxides, which may drive frustrated behavior. Raman signatures of thin film Ba(ZrSnTiHfNb)O_3 show identifying features of random atomic distortions[24] which, in $BaTiO_3$ based ferroelectrics, can be correlated to relaxor-like characteristics[59,60].

A manifestation of charge-lattice coupling in these materials is the exceedingly low thermal transport that approaches the amorphous limit in phase pure, crystalline samples[15,61,62]. The entropy will favor dense phases, which could be linked to short stiff bonds, but uses charge, bond, and mass disorder to quench the thermal conductivity. In HEOs, local chemical and structural disorder, e.g. the frustrated stereochemistry of Cu^{2+} sites, work to scatter phonons and result in short mean-free paths[62] that drop the thermal conductivity to values close to 2 W m^{-1} K^{-1} at room temperature in high-quality, crystalline

specimens. Through a combination of experimental extended X-Ray fine structure (EXAFS) measurements and charge distributions found from density functional theory (DFT) calculations[63], the authors report that the anomalously low thermal conductivity is dominated by Rayleigh scattering from cation sites of differing bond and charge states. From EXAFS, a distortion of the O octahedra about the Co cation sites was observed, which agrees with the observation of charge disorder seen on the Co cation in other works[31] and is complemented by a similar observation of distortion about the Cu site in thin films[21]. All of these works agree that the structural disorder seen in these materials is concentrated on the oxygen sublattice, with the cations remaining in their approximate equilibrium positions. Recent reports of ultra-low thermal conductivity have been observed in other entropy-stabilized crystal structures[64,65] beyond the 5-component rock salt oxides and even other high entropy systems[61,66], which indicates that it may be an intrinsic and emergent property caused by the additional degrees of freedom (charge and structural disorder) in high-entropy materials.

Recently, Brahlek et al. have reported control of concerted orthorhombic structural distortions in $La(CrMnFeCoNi)O_3$ due to competing phases from the constituent B-site cations[67]. Of the bulk oxides, $LaCrO_3$, $LaMnO_3$, and $LaFeO_3$ are orthorhombic, while $LaCoO_3$ and $LaNiO_3$ are rhombohedral due to differences in octahedral tilt angles. This concerted distortion has also been seen in high entropy nickelate $(LaPrNdSmEu)NiO_3$, in which the material goes through a low temperature metal-insulator-transition[23] due to a concerted octahedral rotation, much like the parent rare earth nickelates with the exception of $LaNiO_3$. This transition is structural in nature and agrees with the rule-of-mixtures estimation from the high entropy A-site, importantly showing that existing site-specific correlated phenomena can be preserved in the presence of entropy engineering. The transition, however, is broadened in temperature compared to the parent material, potentially indicating the presence of local variances of the concerted distortion and associated metal-insulator-transition. These works demonstrate that entropy, beyond the creation of new phases, can be a valuable knob to tune structural correlations.

Relatively early in the history of entropy-stabilized oxides, Berardan et al. reported on the observation of a large dielectric constant (order of 10^4) in both (MgCoNiCuZn)O and select compositional variations containing Li and Ga[68]. In these studies, however, the largest dielectric constant lies at frequencies of 1 kHz or less with temperature dependent loss tangents on the order of 1-10 at room temperature. This work was followed up by the same group reporting on the superionic conduction of Li in these same compositions[69], which they attribute to large space created in the lattice by uncorrelated atomic displacements. Since the observation of superionic transport, other works have explored the use of ESOs for battery materials[70–73] and catalysts[74,75], motivated by the material's disordered surface structure and anomalous thermodynamics. More recent studies on the dielectric behavior in perovskite oxides have shown dielectric constants on the order of 40-80 up to approximately 10^6 Hz with much lower loss tangents[76], in the neighborhood of 0.1.

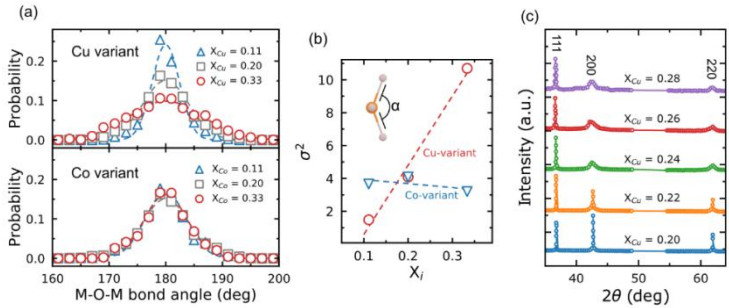

Figure 4: (a) Histogram of the M-O-M bond angle from DFT calculations, showing the change in structural frustration as a function of Cu cation concentration, a Jahn-Teller active cation that will force rhombohedral distortions in the rock salt lattice. **(b)** Plot of the M-O-M bond angle variance, demonstrating the tunability of the structure via stereochemistry of the cation site. **(c)** X-ray diffraction pattern of bulk (MgCoNiCu$_x$Zn)O high entropy oxides while varying the relative composition of Cu. As X_{Cu} increases, the ratio between the 111 and high-symmetry 200 diffraction peaks changes due to the Jahn-Teller distortion effecting the highest symmetry reflection. Parts **(a,b)** from ref [31]. Part **(c)** from ref [58].

Other recent bulk studies on ESOs have explored the possibility that this electronic behavior is partially mediated by oxygen or cation vacancy formation, and the role of such defects in the high entropy system[77–79]. Grzesik and colleagues have concluded that the (MgCoNiCuZn)O ESO lattice can harbor a large number of oxygen defects (up to 7% at equilibrium) which are localized to the cation species which have the largest strain fields and unfavorable local thermodynamics[77,78]. These high number of defects could work in concert with local structural disorder to create sites for electronic and ionic transport, helping to explain the material's conductive-leaning transport properties. This is in agreement with previous work from the high entropy alloy community, which, working with amorphous oxide materials naturally containing a significant number of defects, has observed a very low electrical resistivity[80,81]. Further work on (CeLaPrSmY)O_2 high entropy fluorite has demonstrated that the band gap and crystalline structure of the material can be tuned via the oxygen stoichiometry due to hybridization of the O and rare earth atoms[82].

Magnetism

In oxides, the magnetic exchange between two transition metal cations involves the nonmagnetic oxygen anion as an intermediate. The atomic magnetic moments are realized by the partially filled 3d shell and Hund's exchange. However, the interatomic exchange is mediated through the fully occupied 2*p* shells of the doubly charged O^{2-} anions. The interatomic exchange occurs by the hopping or virtual hopping of electrons between the filled 2*p* shell of the oxygen and the partially occupied 3*d* shell of the transition metal, these are the so-called double exchange and superexchange interactions, respectively. Double exchange can be found in mixed-valence manganites

and leads to ferromagnetic order and conduction[83]. However, superexchange leads to antiferromagnetic or ferrimagnetic insulators which is most prevalent in magnetic oxides. Thus, the superexhange interaction will primarily be our focus. The strength and sign of which is dependent on the degree of 3*d* orbital filling of the metal cations and the bond angle between the 2*p* and 3*d* shells as described by Goodenough-Kanamori-Anderson rules[83–85]. Perhaps most critically for our discussion, as the superexchange interaction is short-range, the emergence of magnetic order is critically dependent on the density of magnetic cations, which must exceed a percolation threshold, and bonding, which can be frustrated by the lattice topology and disorder[31,35,43,86]. Naturally, the magnetic dilution can be changed with composition but the local and global structure of high-entropy oxides can also be tuned through deposition conditions and composition, thus providing pathways to investigate and tune the magnets and roles of disorder in high-entropy systems. Frustrated magnetism has attracted recent study due to the computational applications and rich physics of spin glasses[87,88], spin ices[35,36,89], and spin liquids[37,38]. These phases generally arise due to strong localization of electrons and competing magnetic interactions, such as in a trigonal lattice or between ferromagnetic-antiferromagnetic nearest neighbor exchange[38]. Being a disorder driven physical property, this presents an opportunity for HEOs, as these have already been shown to present concerted phenomena[67], as well as show strongly localized physics[90] and frustrated magnetic interactions[31,47,91]. Below we review recent work that investigates the magnetic ordering and frustration in magnetically dilute entropy-stabilized oxides and its tunability with magnetic dilution and disorder.

The rocksalt (MgCoNiCuZn)O entropy-stabilized oxide consists of three magnetic binary constituents (monoclinically-distorted rocksalt CoO, rhombohedrally-distorted rocksalt NiO, and tenorite/rocksalt CuO). The magnetic order in binary rocksalt oxides with more than half-filled 3d-shells is typically antiferromagnetic due to the strong antiferromagnetic superexchange interaction along the 180° metal-oxygen-metal bonds[83]. This order, however, depends critically on the density of magnetic cations exceeding a percolation threshold and frustration of the antiferromagnetic bonding by lattice topology. In fact, rocksalt CoO, NiO, and CuO are all antiferromagnetic with a strong antiferromagnetic interaction along the 180° metal-oxygen-metal bonds, while tenorite CuO is monoclinic with long range antiferromagnetic order. As only three of the five cations are magnetic and the disorder of the oxygen sublattice due to cation radii differences and the Jahn-Teller distortion from the Cu^{2+} cation[31,32,58] (**Figure 4(a,b)**), the anticipated ground state magnetic order becomes unclear.

Further work from two independent research teams on bulk polycrystalline specimens of (MgCoNiCuZn)O using neutron, X-ray synchrotron, and magnetometry measurements corroborated the prior work and shed new light on the details of the ordering[47,48]. Neutron diffraction revealed ferromagnetic {111} planes that are antiferromagnetically coupled between neighboring planes and magnetic moments oriented along $\langle 11\bar{2} \rangle$ directions. Interestingly, this is the same magnetic order (G-type) observed in NiO. The ordering was found to emerge below ~120 K demonstrating the emergence of long-range G-type antiferromagnetic order with the cation moments oriented along the $\langle 11\bar{2} \rangle$. A sluggish change in the order parameter and the lack of a sharp peak in the heat capacity measurements through the magnetic transition temperature identified by both neutron diffraction[47] (**Figure 5**) and muon spin resonance experiments[91] also indicates a glassy/disorder element to the magnetic transition.

Meisenheimer et al., reported on the magnetic ordering, anisotropy, and ordering temperature in (MgCoNiCuZn)O[19] and compositional variants using thin films. This was done using thin film "exchange bias" heterostructures which consist of a thin soft ferromagnetic layer, such as permalloy (Py), on top of a 70 nm thick (MgCoNiCuZn)O single crystal film. In exchange bias, the hard spins at the surface of the antiferromagnet will interact with the relatively soft spins in the ferromagnetic layer, allowing magnetic information to be read from the AFM using magnetometry. This technique is not only extremely sensitive to disorder, being driven by the uncompensated spins at the surface which are allowed to interact, but is one of the few methods for characterizing insulating thin film antiferromagnets. In these thin film exchange coupling measurements, the magnetic order and ordering temperature can be inferred by the modification of the soft ferromagnet's anisotropy at the onset of magnetic ordering in the oxide layer[31,92,93]. This coupling manifests as a broadening (coercivity enhancement) and horizontal shift (exchange bias) of the soft magnet's hysteresis loop as well as a divergence of the field cool and zero field cool moment versus temperature curves at the ordering temperature.

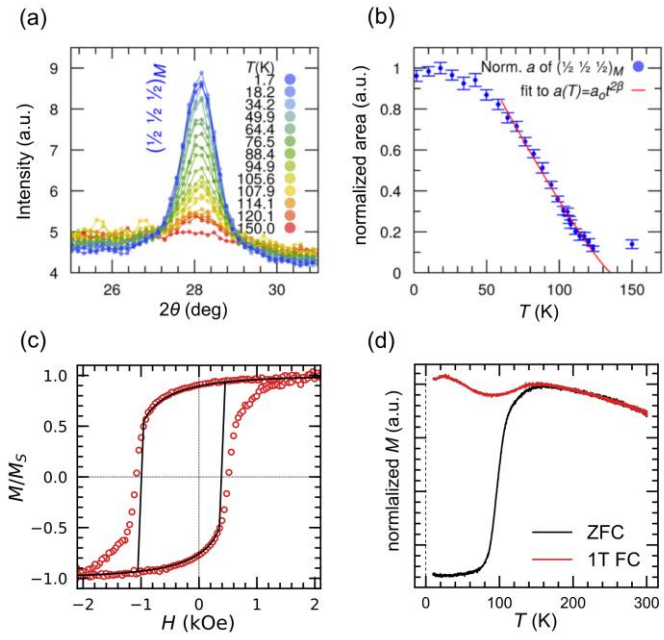

Figure 5: (a) Neutron diffraction spectrum of a bulk sample showing the development of the [½ ½ ½] magnetic diffraction peak across the Neel temperature. **(b)** Normalized area of the peak in (c), showing the same long glass-like transition to the antiferromagnetic state. **(c)** Exchange biased hysteresis loop from thin film permalloy/(MgCoNiCuZn)O at 10 K along [100] showing that it is antiferromagnetic with a large uncompensated moment. **(d)** Moment versus temperature curve of the same sample, showing the long, glassy transition to the antiferromagnetic state. **(a,b)** from ref [47] **(c,d)** from ref [31].

Temperature dependent magnetometry measurements of the heterostructure performed along differing crystallographic direction reveal long range antiferromagnetic order in the entropy-stabilized oxide below ~165 K[19]. The antiferromagnetic nature of the oxide is made from the observation of anisotropic magnetic exchange bias between the [100] and [110] directions and the exchange coupling disappearing at the ordering temperature. It was also observed that the exchange bias observed at low temperature reached ~10x the exchange bias observed in a CoO/Py control sample. Exchange bias is mediated by pinned uncompensated spins in the antiferromagnetic layer at or near the interface. Thus the inclusions of non-magnetic cations and structural disorder may be responsible for this extreme behavior[31].

The magnetic properties have been characterized in other oxide crystal structures including spinels[94–96] and perovskites[25,90]. In spinels, the Néel temperature and magnetic saturation tends to follow continuum trends, where as the magnetic lattice is diluted, the ferrimagnetic transition temperature and the saturation magnetization both decrease. Ferrite-based spinels of the type $(MgCoNiCuZn)Fe_2O_4$ tend to be magnetically soft, with coercive fields on the order of ~ 100 Oe, whereas, more interestingly, chromite-based spinels are much harder, with coercive fields on the order of as much as 1 T, and display magnetic inconsistencies that belie their glassy nature. For example, $(MgCoFeNiCu)Cr_2O_4$ spinels show a large field dependent Néel temperature and magnetization, which changes from 70-120 K under different training fields[96] (cooled in 1000 Oe and 100 Oe respectively). Musicó and colleagues attribute this observation to the existence of ferromagnetic regions before the critical temperature which, when saturated, increase the net magnetization and compete with overall ferrimagnetic order.

A similar result is reported for $La(CrMnFeCoNi)O_3$-type perovskites, where an intrinsic exchange bias-like effect is attributed to the formation of small local ferromagnetic regions contributing to the magnetization. The authors confirm this using Mossbauer spectroscopy, showing that the Fe moments in the HEO are in a mix of ferromagnetic and antiferromagnetic states (**Figure 6**) caused by competing superexchange and double exchange reactions between neighboring cations[90]. This is an exciting result because it is directly analogous to the formation of ferroelectric PNR discussed above, providing evidence that these magnetically analogous phenomena may be possible in an HEO and indicating the presence of competing ferroic orders. It was also found that, as the A site cation size changes and the structure deviates away from the ideal cubic perovskite, the frustration of the magnetic lattice (read through the Néel temperature) increases in a quasilinear manner. It is argued that this is due to increasing frustration of the octahedral cage, paralleling the complementary result found in the seminal ESO rock salt in reference [31]. When these same materials were deposited as single crystalline films with varying strain states[25], it was found that saturation magnetization scales with the in-plane strain, seemingly supporting this conclusion. These observations provide evidence of frustrated and disordered magnetism in HEOs, with direct analogues to existing relaxor materials. This indicates that engineering of the magnetic phase in HEOs should be achievable with both new and existing synthesis techniques. In the short term, the natural extension of these materials to frustrated magnetic systems such as spin glasses and liquids is promising.

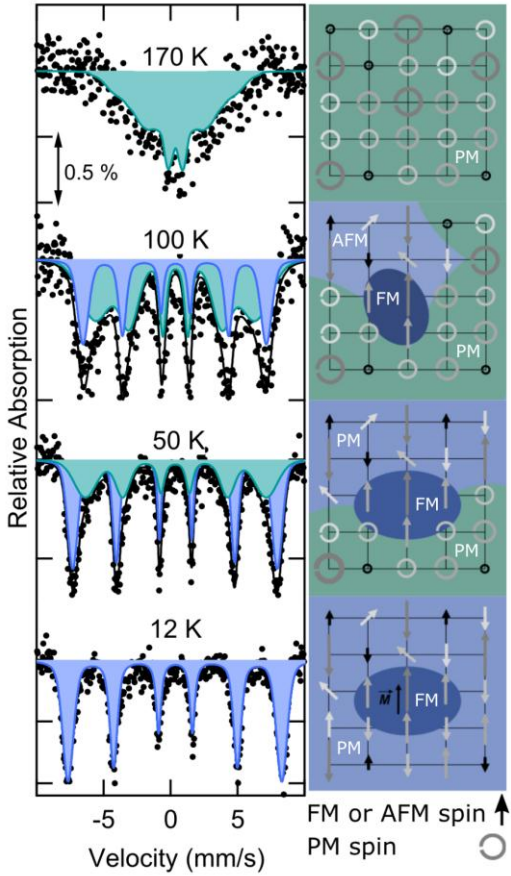

Figure 6: Fe Mossbauer spectroscopy showing the magnetic structure of La(CrMnFeCoNi)O_3 below the Neel temperature, in which ferromagnetic nanoclusters are embedded in the antiferromagnetic (AFM)/Paramagnetic (PM) matrix through the broad transition. From ref [90].

Frustrated magnetism in spin glasses has been targeted due to its similarity to biological computing, with the study of spin glasses spurring advancement in the fields of neuromorphic computing and machine learning[87,97–99]. This is because a magnetically frustrated system, caused by competing ferromagnetic and antiferromagnetic interactions within the material, has a large number of possible frozen metastable states, with coherence times that can be on the order of hours to days[88,100]. As the materials is cooled below its transition temperature, the spins will freeze into a disordered configuration that is not only a function of the input (magnetic field, cooling rate, etc.) but will still respond slowly to an external stimulus. Due to a nonlinear phase response (i.e. a different frozen spin configuration due to differences in magnetic field, cooling temperature, time, etc.), these systems have long been used to understand processes of neural network computing[101,102] and dynamics in other metastable-phase analogs[88,103–105].

From a materials perspective, these materials can be characterized by a frequency dependent response to AC magnetic field (much like relaxor ferroelectrics), long, field dependent transition periods, and slow, nonlinear time evolution[44,106–108]. This glassy response to magnetic field has been observed in bulk antiferromagnetic ESOs[47] (in Li containing rocksalt oxides), where a small frequency dependence was seen in in the transition temperature between 100 Hz and 10 kHz. This should be a natural extrapolation of the current knowledge about magnetism in these materials, as local superexchange interactions will compete between ferromagnetic and antiferromagnetic depending on the neighboring species[19,90]. Theoretical work[109] on (MgCoNiCuZn)O observes that the dilute magnetism in these materials behaves much like their antiferromagnetic rock salt counterparts CoO and NiO, which go through multiple magnetic phase transitions as the cation lattice is diluted with diamagnetic species[110,111]. As both of these materials demonstrate frustrated AFM and true spin glass regions, it is reasonable to conclude that this same phenomena is reproducible in the HEO. Indeed this idea of using exchange bias from a spin glass to explore and tune the magnetic disorder in the system was explored recently[31], showing that the magnetic exchange in these materials can be controlled over a very large range, opening a pathway for further understanding of these phenomena.

HEOs is a nascent field and guidance can be drawn from the high-entropy alloy (HEA) community that has existed for close to 20 years. Much of the work in HEAs is concerned with mechanical behavior[2,6,10,112,113], however, there exists a body of work on magnetism[114–116], phase stability[117,118], and defect formation/transport[119,120] that is directly relatable to discussions on correlated materials. For instance, it has been observed in HEA CoCrMnFeNi that a FCC-HCP phase change can be driven using high magnetic field[118], showing a distinct spin-lattice coupling that may be valuable to the study of disordered magnetic materials. HEOs have been composed of constituents with different structures and magnetic interactions, however the potential structural and magnetic diversity within existing transition metal HEAs is much greater than the HEOs studied currently. Expanding the number of competing magnetic and structural parent phases should increase frustration and potentially create nearly degenerate ground states for the formation of spin glasses, ices, and liquids or controllable phase transitions.

This paradigm can be further extended to glassy networks of other ferroic properties beyond magnetic spin glasses (analogous to ferromagnets), including strain glasses[121,122] (analogous to ferroelastics), dipole glasses[123,124] (ferroelectrics), and multiglasses with multiple coupled glassy ferroic orders[125–128]. Because of the natural disorder in entropy-stabilized materials, this looks to be the logical progression towards the synthesis of crystals with true ferroic orders.

CONCLUDING REMARKS AND OUTLOOK

HEOs are an emerging field of materials that show significant promise, not only for mechanical applications[62,64], but for correlated electron behavior, a field where oxides display a wide range of fantastic properties[34,37,49,52]. A significant draw of high-entropy effects is the enhanced solubilities of typically immiscible cations, which allows for stabilization of species in typically unfavorable environments due to competing stereochemistry[31,32,58], charge[62,63], or magnetic ordering[47,48,109]. This effect can even be further extended by carefully controlling the kinetics with modern materials techniques such as nanoparticle synthesis or PVD, further extending the potential phase space of these many-component materials and offering an unparalleled tunability of charge, spin,

orbital, and lattice degrees of freedom. Combined with the fact that oxides already offer an exciting playground for the study of new physical phenomena and technologically important properties, the advancement of the field is a direct opportunity for engineering and studying HEOs as an avenue for correlated electron systems.

One of the most important points for disorder driven functional phenomena is frustration of the order parameter, such as the competition of ferroelectricity/antiferroelectricity, resulting in relaxor behavior, and ferromagnetism/antiferromagnetism which drives magnetic glassiness. Recent studies in HEOs have demonstrated this ferroic frustration in magnetic systems[19,31,47,48,91], as well as to a limited extent structurally in perovskite oxides[23,24]. Due to the large number of competing cation neighbors, these materials seem to be a model system for the demonstration of frustrated ferroic phenomena like strain, dipole, and spin glassiness. In addition to their unprecedented structural tunability[19,22–24] HEOs display the ability to be grown on a variety of substrates[15,25], including amorphous materials, resulting in a substrate versatility for potential applications. This combined with their relatively low deposition temperatures may make these materials extremely valuable for the electronics industry.

There are still a number of questions to be answered about HEOs, namely the role of disorder in functional phenomena[31,62], the role of defects[77,78], and the stability of new phases and compositions[129,130]. Though the field is still developing, inspiration can come from existing work on functionality in the high-entropy alloy community on magnetism[114–116], defect formation/transport[119,120], and phase stability[117,118]. HEOs have the exciting potential to become an extremely functionally relevant class of materials by incorporating new methods to enhance solubility and disorder with existing materials synthesis knowledge and techniques.

ACKNOWLEDGEMENTS

This work was supported by NSF CAREER grant DMR-1847847.

References

[1] J.W. Yeh, S.K. Chen, S.J. Lin, J.Y. Gan, T.S. Chin, T.T. Shun, C.H. Tsau, and S.Y. Chang, Advanced Engineering Materials **6**, 299 (2004).
[2] D.B. Miracle, JOM 1 (2017).
[3] M.-H. Tsai and J.-W. Yeh, Materials Research Letters **2**, 107 (2014).
[4] M.-H. Tsai, Entropy **15**, 5338 (2013).
[5] F. Otto, Y. Yang, H. Bei, and E.P. George, Acta Materialia **61**, 2628 (2013).
[6] M.C. Gao, C.S. Carney, N. Dogan, P.D. Jablonksi, J.A. Hawk, and D.E. Alman, Jom **67**, 2653 (2015).
[7] Y.P. Wang, B.S. Li, and H.Z. Fu, Advanced Engineering Materials **11**, 641 (2009).
[8] X. Ji, International Journal of Cast Metals Research **28**, 229 (2015).
[9] C.M. Rost, E. Sachet, T. Borman, A. Moballegh, E.C. Dickey, D. Hou, J.L. Jones, S. Curtarolo, and J.-P. Maria, Nature Communications **6**, 8485 (2015).
[10] B. Gludovatz, A. Hohenwarter, D. Catoor, E.H. Chang, E.P. George, and R.O. Ritchie, Science **345**, 1153 (2014).
[11] A.D. Pogrebnjak, I.V. Yakushchenko, G. Abadias, P. Chartier, O.V. Bondar, V.M. Beresnev, Y. Takeda, O.V. Sobol', K. Oyoshi, A.A. Andreyev, and B.A. Mukushev, J. Superhard Mater. **35**, 356 (2013).

[12] F. Meng and I. Baker, Journal of Alloys and Compounds **645**, 376 (2015).
[13] A.D. Pogrebnjak, A.A. Bagdasaryan, I.V. Yakushchenko, and V.M. Beresnev, Russ. Chem. Rev. **83**, 1027 (2014).
[14] B.L. Musicó, D. Gilbert, T.Z. Ward, K. Page, E. George, J. Yan, D. Mandrus, and V. Keppens, APL Materials **8**, 040912 (2020).
[15] G.N. Kotsonis, C.M. Rost, D.T. Harris, and J.-P. Maria, MRS Communications **8**, 1371 (2018).
[16] A. Sarkar, R. Djenadic, N.J. Usharani, K.P. Sanghvi, V.S.K. Chakravadhanula, A.S. Gandhi, H. Hahn, and S.S. Bhattacharya, Journal of the European Ceramic Society **37**, 747 (2017).
[17] D. Liu, X. Peng, J. Liu, L. Chen, Y. Yang, and L. An, Journal of the European Ceramic Society **40**, 2504 (2020).
[18] C. Rost, Entropy-Stabilized Oxides: Explorations of a Novel Class of Multicomponent Materials, North Carolina State University, 2016.
[19] P.B. Meisenheimer, T.J. Kratofil, and J.T. Heron, Scientific Reports **7**, 13344 (2017).
[20] S. Sivakumar, E. Zwier, P.B. Meisenheimer, and J.T. Heron, JoVE (Journal of Visualized Experiments) e57746 (2018).
[21] C.M. Rost, Z. Rak, D.W. Brenner, and J.-P. Maria, Journal of the American Ceramic Society **100**, 2732 (n.d.).
[22] B.D. Esser, A.J. Hauser, R.E.A. Williams, L.J. Allen, P.M. Woodward, F.Y. Yang, and D.W. McComb, Phys. Rev. Lett. **117**, 176101 (2016).
[23] R.K. Patel, S.K. Ojha, S. Kumar, A. Saha, P. Mandal, J.W. Freeland, and S. Middey, Applied Physics Letters **116**, 071601 (2020).
[24] Y. Sharma, B.L. Musico, X. Gao, C. Hua, A.F. May, A. Herklotz, A. Rastogi, D. Mandrus, J. Yan, H.N. Lee, M.F. Chisholm, V. Keppens, and T.Z. Ward, Phys. Rev. Materials **2**, 060404 (2018).
[25] Y. Sharma, Q. Zheng, A.R. Mazza, E. Skoropata, T. Heitmann, Z. Gai, B. Musico, P.F. Miceli, B.C. Sales, V. Keppens, M. Brahlek, and T.Z. Ward, Phys. Rev. Materials **4**, 014404 (2020).
[26] J. Assal, B. Hallstedt, and L.J. Gauckler, Zeitschrift Fuer Metallkunde **87**, (1996).
[27] L.A. Zabdyr and O.B. Fabrichnaya, JPE **23**, 149 (2002).
[28] P. Perrot and H. Kumar, *Cu-Ni-O Ternary Phase Diagram Evaluation* (MSI Materials Science International Services GmbH, Stuttgart, n.d.).
[29] J.F. Sarver, F.L. Katnack, and F.A. Hummel, J. Electrochem. Soc. **106**, 960 (1959).
[30] C.H. Bates, W.B. White, and R. Roy, Journal of Inorganic and Nuclear Chemistry **28**, 397 (1966).
[31] P.B. Meisenheimer, L.D. Williams, S.H. Sung, J. Gim, P. Shafer, G.N. Kotsonis, J.-P. Maria, M. Trassin, R. Hovden, E. Kioupakis, and J.T. Heron, Phys. Rev. Materials **3**, 104420 (2019).
[32] Zs. Rák, J.-P. Maria, and D.W. Brenner, Materials Letters **217**, 300 (2018).
[33] L.W. Martin, Y.-H. Chu, and R. Ramesh, Materials Science and Engineering: R: Reports **68**, 89 (2010).
[34] R. Ramesh and N.A. Spaldin, Nature Materials **6**, 21 (2007).
[35] S.T. Bramwell and M.J.P. Gingras, Science **294**, 1495 (2001).
[36] A.P. Ramirez, A. Hayashi, R.J. Cava, R. Siddharthan, and B.S. Shastry, Nature **399**, 333 (1999).
[37] C. Broholm, R.J. Cava, S.A. Kivelson, D.G. Nocera, M.R. Norman, and T. Senthil, Science **367**, (2020).
[38] L. Balents, Nature **464**, 199 (2010).
[39] D. Dijkkamp, T. Venkatesan, X.D. Wu, S.A. Shaheen, N. Jisrawi, Y.H. Min-Lee, W.L. McLean, and M. Croft, Appl. Phys. Lett. **51**, 619 (1987).
[40] W.E. Pickett, Rev. Mod. Phys. **61**, 433 (1989).
[41] P.M. Grant, J. Phys.: Conf. Ser. **129**, 012042 (2008).
[42] J.A. Mundy, C.M. Brooks, M.E. Holtz, J.A. Moyer, H. Das, A.F. Rébola, J.T. Heron, J.D. Clarkson, S.M. Disseler, Z. Liu, A. Farhan, R. Held, R. Hovden, E. Padgett, Q. Mao, H. Paik, R. Misra, L.F. Kourkoutis, E. Arenholz, A. Scholl, J.A. Borchers, W.D. Ratcliff, R. Ramesh, C.J.

Fennie, P. Schiffer, D.A. Muller, and D.G. Schlom, Nature **537**, 523 (2016).
[43] M.W. Lufaso and P.M. Woodward, Acta Cryst B, Acta Cryst Sect B, Acta Crystallogr B, Acta Crystallogr Sect B, Acta Crystallogr Struct Sci, Acta Crystallogr Sect B Struct Sci, Acta Crystallogr B Struct Sci Cryst Eng Mater **60**, 10 (2004).
[44] J.F. Ding, O.I. Lebedev, S. Turner, Y.F. Tian, W.J. Hu, J.W. Seo, C. Panagopoulos, W. Prellier, G. Van Tendeloo, and T. Wu, Phys. Rev. B **87**, 054428 (2013).
[45] M. Bibes, J.E. Villegas, and A. Barthélémy, Advances in Physics **60**, 5 (2011).
[46] M.D. Biegalski, Y. Jia, D.G. Schlom, S. Trolier-McKinstry, S.K. Streiffer, V. Sherman, R. Uecker, and P. Reiche, Appl. Phys. Lett. **88**, 192907 (2006).
[47] M.P. Jimenez-Segura, T. Takayama, D. Bérardan, A. Hoser, M. Reehuis, H. Takagi, and N. Dragoe, Appl. Phys. Lett. **114**, 122401 (2019).
[48] J. Zhang, J. Yan, S. Calder, Q. Zheng, M.A. McGuire, D.L. Abernathy, Y. Ren, S.H. Lapidus, K. Page, H. Zheng, J.W. Freeland, J.D. Budai, and R.P. Hermann, Chem. Mater. **31**, 3705 (2019).
[49] M.J. Krogstad, P.M. Gehring, S. Rosenkranz, R. Osborn, F. Ye, Y. Liu, J.P.C. Ruff, W. Chen, J.M. Wozniak, H. Luo, O. Chmaissem, Z.-G. Ye, and D. Phelan, Nature Materials 1 (2018).
[50] Z.-Y. Cheng, R.S. Katiyar, X. Yao, and A.S. Bhalla, Phys. Rev. B **57**, 8166 (1998).
[51] L.E. Cross, Ferroelectrics **76**, 241 (1987).
[52] D. Damjanovic, Rep. Prog. Phys. **61**, 1267 (1998).
[53] I. Grinberg, V.R. Cooper, and A.M. Rappe, Nature **419**, 909 (2002).
[54] I. Grinberg, V.R. Cooper, and A.M. Rappe, Phys. Rev. B **69**, 144118 (2004).
[55] M. Eremenko, V. Krayzman, A. Bosak, H.Y. Playford, K.W. Chapman, J.C. Woicik, B. Ravel, and I. Levin, Nat Commun **10**, 1 (2019).
[56] M.E. Manley, D.L. Abernathy, R. Sahul, D.E. Parshall, J.W. Lynn, A.D. Christianson, P.J. Stonaha, E.D. Specht, and J.D. Budai, Science Advances **2**, e1501814 (2016).
[57] F. Li, S. Zhang, T. Yang, Z. Xu, N. Zhang, G. Liu, J. Wang, J. Wang, Z. Cheng, Z.-G. Ye, J. Luo, T.R. Shrout, and L.-Q. Chen, Nat Commun **7**, 1 (2016).
[58] D. Berardan, A.K. Meena, S. Franger, C. Herrero, and N. Dragoe, Journal of Alloys and Compounds **704**, 693 (2017).
[59] A. Dixit, S.B. Majumder, R.S. Katiyar, and A.S. Bhalla, J Mater Sci **41**, 87 (2006).
[60] Y.-S. Seo, J.S. Ahn, and I.-K. Jeong, Journal of the Korean Physical Society **62**, 749 (2013).
[61] J. Gild, Y. Zhang, T. Harrington, S. Jiang, T. Hu, M.C. Quinn, W.M. Mellor, N. Zhou, K. Vecchio, and J. Luo, Scientific Reports **6**, 37946 (2016).
[62] J.L. Braun, C.M. Rost, M. Lim, A. Giri, D.H. Olson, G.N. Kotsonis, G. Stan, D.W. Brenner, J.-P. Maria, and P.E. Hopkins, Advanced Materials **30**, 1805004 (2018).
[63] Zs. Rak, C.M. Rost, M. Lim, P. Sarker, C. Toher, S. Curtarolo, J.-P. Maria, and D.W. Brenner, Journal of Applied Physics **120**, 095105 (2016).
[64] F. Li, L. Zhou, J.-X. Liu, Y. Liang, and G.-J. Zhang, J Adv Ceram **8**, 576 (2019).
[65] J. Gild, M. Samiee, J.L. Braun, T. Harrington, H. Vega, P.E. Hopkins, K. Vecchio, and J. Luo, Journal of the European Ceramic Society **38**, 3578 (2018).
[66] X. Yan, L. Constantin, Y. Lu, J.-F. Silvain, M. Nastasi, and B. Cui, Journal of the American Ceramic Society **101**, 4486 (2018).
[67] M. Brahlek, A.R. Mazza, K.C. Pitike, E. Skoropata, J. Lapano, G. Eres, V.R. Cooper, and T.Z. Ward, ArXiv:2004.02985 [Cond-Mat] (2020).
[68] D. Berardan, S. Franger, D. Dragoe, A.K. Meena, and N. Dragoe, Physica Status Solidi - Rapid Research Letters **10**, 328 (2016).
[69] D. Berardan, S. Franger, A.K. Meena, and N. Dragoe, J. Mater. Chem. A 9536 (2016).

[70] A. Sarkar, L. Velasco, D. Wang, Q. Wang, G. Talasila, L. de Biasi, C. Kübel, T. Brezesinski, S.S. Bhattacharya, H. Hahn, and B. Breitung, Nat Commun **9**, 1 (2018).
[71] N. Qiu, H. Chen, Z. Yang, S. Sun, Y. Wang, and Y. Cui, Journal of Alloys and Compounds **777**, 767 (2019).
[72] Q. Wang, A. Sarkar, Z. Li, Y. Lu, L. Velasco, S.S. Bhattacharya, T. Brezesinski, H. Hahn, and B. Breitung, Electrochemistry Communications **100**, 121 (2019).
[73] Y. Zheng, Y. Yi, M. Fan, H. Liu, X. Li, R. Zhang, M. Li, and Z.-A. Qiao, Energy Storage Materials **23**, 678 (2019).
[74] H. Chen, J. Fu, P. Zhang, H. Peng, C.W. Abney, K. Jie, X. Liu, M. Chi, and S. Dai, J. Mater. Chem. A **6**, 11129 (2018).
[75] H. Chen, W. Lin, Z. Zhang, K. Jie, D.R. Mullins, X. Sang, S.-Z. Yang, C.J. Jafta, C.A. Bridges, X. Hu, R.R. Unocic, J. Fu, P. Zhang, and S. Dai, ACS Materials Lett. **1**, 83 (2019).
[76] Q. Du, J. Yan, X. Zhang, J. Li, X. Liu, J. Zhang, and X. Qi, J Mater Sci: Mater Electron (2020).
[77] Z. Grzesik, G. Smoła, M. Stygar, J. Dąbrowa, M. Zajusz, K. Mroczka, and M. Danielewski, Journal of the European Ceramic Society **39**, 4292 (2019).
[78] L.K. Bhaskar, V. Nallathambi, and R. Kumar, Journal of the American Ceramic Society **103**, 3416 (2020).
[79] M.-I. Lin, M.-H. Tsai, W.-J. Shen, and J.-W. Yeh, Thin Solid Films **518**, 2732 (2010).
[80] C.-H. Tsau, Y.-C. Yang, C.-C. Lee, L.-Y. Wu, and H.-J. Huang, Procedia Engineering **36**, 246 (2012).
[81] C.-H. Tsau, Z.-Y. Hwang, and S.-K. Chen, Advances in Materials Science and Engineering **2015**, (2015).
[82] A. Sarkar, B. Eggert, L. Velasco, X. Mu, J. Lill, K. Ollefs, S.S. Bhattacharya, H. Wende, R. Kruk, R.A. Brand, and H. Hahn, ArXiv:2003.00268 [Cond-Mat] (2020).
[83] J.B. Goodenough, Phys. Rev. **100**, 564 (1955).
[84] J. Kanamori, Journal of Physics and Chemistry of Solids **10**, 87 (1959).
[85] P.W. Anderson, Phys. Rev. **79**, 350 (1950).
[86] J.M. Iwata-Harms, F.J. Wong, U.S. Alaan, B.J. Kirby, J.A. Borchers, M.F. Toney, B.B. Nelson-Cheeseman, M. Liberati, E. Arenholz, and Y. Suzuki, Phys. Rev. B **85**, 214424 (2012).
[87] D. Sherrington, in *North-Holland Mathematical Library*, edited by J.G. Taylor (Elsevier, 1993), pp. 261–291.
[88] G. Parisi, Proceedings of the National Academy of Sciences **103**, 7948 (2006).
[89] R.F. Wang, C. Nisoli, R.S. Freitas, J. Li, W. McConville, B.J. Cooley, M.S. Lund, N. Samarth, C. Leighton, V.H. Crespi, and P. Schiffer, Nature **439**, 303 (2006).
[90] R. Witte, A. Sarkar, R. Kruk, B. Eggert, R.A. Brand, H. Wende, and H. Hahn, Phys. Rev. Materials **3**, 034406 (2019).
[91] B.A. Frandsen, K.A. Petersen, N.A. Ducharme, A.G. Shaw, E.J. Gibson, B. Winn, J. Yan, J. Zhang, M.E. Manley, and R.P. Hermann, ArXiv:2004.04218 [Cond-Mat] (2020).
[92] F. Radu and H. Zabel, Springer Tracts in Modern Physics **227**, 97 (2007).
[93] J.T. Heron, M. Trassin, K. Ashraf, M. Gajek, Q. He, S.Y. Yang, D.E. Nikonov, Y.H. Chu, S. Salahuddin, and R. Ramesh, Physical Review Letters **107**, 1 (2011).
[94] A. Mao, H.-Z. Xiang, Z.-G. Zhang, K. Kuramoto, H. Zhang, and Y. Jia, Journal of Magnetism and Magnetic Materials **497**, 165884 (2020).
[95] A. Mao, H.-X. Xie, H.-Z. Xiang, Z.-G. Zhang, H. Zhang, and S. Ran, Journal of Magnetism and Magnetic Materials **503**, 166594 (2020).
[96] B. Musicó, Q. Wright, T.Z. Ward, A. Grutter, E. Arenholz, D. Gilbert, D. Mandrus, and V. Keppens, Phys. Rev. Materials **3**, 104416 (2019).
[97] D.J. Amit, H. Gutfreund, and H. Sompolinsky, Phys. Rev. A **32**, 1007 (1985).
[98] P. Baldi and S.S. Venkatesh, Phys. Rev. Lett. **58**, 913 (1987).

[99] K.E. Hamilton, C.D. Schuman, S.R. Young, N. Imam, and T.S. Humble, in *2018 IEEE International Parallel and Distributed Processing Symposium Workshops (IPDPSW)* (2018), pp. 1194–1203.
[100] F. Bert, V. Dupuis, E. Vincent, J. Hammann, and J.-P. Bouchaud, Phys. Rev. Lett. **92**, 167203 (2004).
[101] G. Parisi, Physica A: Statistical Mechanics and Its Applications **194**, 28 (1993).
[102] G. Parisi and F. Slanina, EPL **17**, 497 (1992).
[103] M. Mézard and G. Parisi, J. Phys.: Condens. Matter **11**, A157 (1999).
[104] D.L. Sidebottom, Front. Mater. **6**, (2019).
[105] C. Yildirim, J.-Y. Raty, and M. Micoulaut, Nat Commun **7**, (2016).
[106] M. Gruyters, Phys. Rev. Lett. **95**, 077204 (2005).
[107] J.-W. Cai, C. Wang, B.-G. Shen, J.-G. Zhao, and W.-S. Zhan, Appl. Phys. Lett. **71**, 1727 (1997).
[108] M. Ali, P. Adie, C.H. Marrows, D. Greig, B.J. Hickey, and R.L. Stamps, Nat Mater **6**, 70 (2007).
[109] Zs. Rák and D.W. Brenner, Journal of Applied Physics **127**, 185108 (2020).
[110] A.Z. Menshikov, Y.A. Dorofeev, A.G. Klimenko, and N.A. Mironova, Physica Status Solidi (b) **164**, 275 (1991).
[111] M.S. Seehra, J.C. Dean, and R. Kannan, Phys. Rev. B **37**, 5864 (1988).
[112] S. Praveen and H.S. Kim, Advanced Engineering Materials **20**, 1700645 (n.d.).
[113] H. Huang, Y. Wu, J. He, H. Wang, X. Liu, K. An, W. Wu, and Z. Lu, Advanced Materials **29**, 1701678 (2017).
[114] M. Acet, AIP Advances **9**, 095037 (2019).
[115] P. Li, A. Wang, and C.T. Liu, Journal of Alloys and Compounds **694**, 55 (2017).
[116] O. Schneeweiss, M. Friák, M. Dudová, D. Holec, M. Šob, D. Kriegner, V. Holý, P. Beran, E.P. George, J. Neugebauer, and A. Dlouhý, Phys. Rev. B **96**, 014437 (2017).
[117] X. Chang, M. Zeng, K. Liu, and L. Fu, Advanced Materials **n/a**, 1907226 (n.d.).
[118] C. Niu, C.R. LaRosa, J. Miao, M.J. Mills, and M. Ghazisaeidi, Nature Communications **9**, 1 (2018).
[119] J. Dąbrowa and M. Danielewski, Metals **10**, 347 (2020).
[120] V. Maier-Kiener, B. Schuh, E.P. George, H. Clemens, and A. Hohenwarter, Journal of Materials Research **32**, 2658 (2017).
[121] S. Sarkar, X. Ren, and K. Otsuka, Phys. Rev. Lett. **95**, 205702 (2005).
[122] Y. Wang, X. Ren, K. Otsuka, and A. Saxena, Phys. Rev. B **76**, 132201 (2007).
[123] S. Iida and H. Terauchi, J. Phys. Soc. Jpn. **52**, 4044 (1983).
[124] B.E. Vugmeister and M.D. Glinchuk, Rev. Mod. Phys. **62**, 993 (1990).
[125] D. Choudhury, P. Mandal, R. Mathieu, A. Hazarika, S. Rajan, A. Sundaresan, U.V. Waghmare, R. Knut, O. Karis, P. Nordblad, and D.D. Sarma, Phys. Rev. Lett. **108**, 127201 (2012).
[126] W. Kleemann, S. Bedanta, P. Borisov, V.V. Shvartsman, S. Miga, J. Dec, A. Tkach, and P.M. Vilarinho, Eur. Phys. J. B **71**, 407 (2009).
[127] W. Kleemann, V.V. Shvartsman, S. Bedanta, P. Borisov, A. Tkach, and P.M. Vilarinho, J. Phys.: Condens. Matter **20**, 434216 (2008).
[128] V.V. Shvartsman, S. Bedanta, P. Borisov, W. Kleemann, A. Tkach, and P.M. Vilarinho, Phys. Rev. Lett. **101**, 165704 (2008).
[129] K. Kaufmann, D. Maryanovsky, W.M. Mellor, C. Zhu, A.S. Rosengarten, T.J. Harrington, C. Oses, C. Toher, S. Curtarolo, and K.S. Vecchio, Npj Computational Materials **6**, 1 (2020).
[130] P. Sarker, T. Harrington, C. Toher, C. Oses, M. Samiee, J.-P. Maria, D.W. Brenner, K.S. Vecchio, and S. Curtarolo, Nat Commun **9**, 1 (2018).